Published in final edited form as:
Mol Cell Neurosci. 2011 May ; 47(1): 1–9. doi:10.1016/j.mcn.2010.12.006.

SCHWANNOMIN/MERLIN PROMOTES SCHWANN CELL ELONGATION AND INFLUENCES MYELIN SEGMENT LENGTH

Courtney Thaxton[a], **Marga Bott**[a], **Barbara Walker**[b], **Nicklaus A. Sparrow**[a], **Stephen Lambert**[b,*], and **Cristina Fernandez-Valle**[*,a,§]

[a]Department of Molecular Biology and Microbiology, Burnett School of Biomedical Science, College of Medicine, University of Central Florida, Health Science Campus, 6900 Lake Nona Boulevard, Orlando, FL 32827

[b]Department of Cell Biology, University of Massachusetts Medical School, 55 Lake Ave. North Worcester, MA 01655-0106

Abstract

The Neurofibromatosis type 2 tumor suppressor, schwannomin (Sch) is a plasma membrane-cytoskeleton linking protein that regulates receptor signaling and actin dynamics. We examined Sch's role in specifying morphological changes needed for Schwann cell (SC) function *in vitro*. Isolated Sch-GFP-expressing SCs extended bipolar processes 82% longer than those formed by GFP-expressing cells. In contrast, SCs expressing dominant negative Sch-BBA-GFP extended bipolar processes 16% shorter than controls and 64% shorter than Sch-GFP-expressing SCs. *nf2* gene inactivation caused isolated mouse SCs to transition from bipolar to multipolar cells. Live imaging revealed that SCs co-expressing Sch-GFP and dominant negative RacN17 behaved similarly in dorsal root ganglion explant cultures; they quickly aligned on axons and slowly elongated bipolar processes. In contrast, SCs expressing constitutively active RacV12 underwent continuous transitions in morphology that interfered with axon alignment. When co-cultured with neurons under myelin-promoting conditions, Sch-GFP-expressing SCs elaborated longer myelin segments than GFP-expressing SCs. In contrast, Sch-BBA-GFP-expressing SCs failed to align on or myelinate axons. Together, these results demonstrate that Sch plays an essential role in inducing and/or maintaining the SC's spindle shape and suggest that the mechanism involves Sch-dependent inhibition of Rac activity. By stabilizing the bipolar morphology, Sch promotes alignment of SCs with axons and ultimately influences myelin segment length.

[§]Corresponding Author: Cristina Fernandez-Valle. University of Central Florida, Health Science Campus, 6900 Lake Nona Boulevard, Orlando, FL 32827. Phone: 407-266-7033. cfernand@mail.ucf.edu Fax: 407 266-7002.
SL is now at College of Medicine, University of Central Florida
[*]Both laboratories contributed equally to this work.

Supplemental Data, Movies 1-3. 21 day-old embryonic rat DRG explant cultures were transfected with plasmids encoding GFP and HA-tagged constitutively active RacV12 (Movie 1), dominant negative RacN17 (Movie 2), and Sch-GFP (Movie 3). 36 hours after transfection, GFP-expressing cells were subjected to real-time fluorescence video imaging for 18 hours. Typically 4-5 random locations were imaged for each transfection in each of 3 independent experiments such that the dynamics of >40 cells/transfection were examined. Behaviors shown were typical for the construct transfected. Images were collected every 5 minutes for 18 hours; the first 10 hours are shown. Image sequences were compressed such that 1 second represents 25 minutes in real time.

Keywords

Schwannomin; myelin; Cdc42; Rac; NF2; Neurofibromatosis

1. INTRODUCTION

Dynamic control of Schwann cell (SC) morphology is critical at all stages of development of the peripheral nervous system. SCs undergo morphological transitions as they develop from immature to myelinating glial cells. The major stages of SC development requiring extensive cytoskeletal remodeling include: 1) radial sorting of axons by extension of multiple processes into axon fascicles, 2) bipolar elongation of processes along axons to establish the presumptive myelin internode, and 3) active myelination by elaboration of a large plasma membrane sheath around axons. The transition from axial elongation along an axon to radial expansion of membrane around an axon represents the most pronounced reorganization of the SC cytoskeleton. How actin polymerization is regulated in SCs during these stages of development is not well understood. However, it must be linked to receptor-dependent mechanisms activated by contact of SCs with axons and extracellular matrix.

The Neurofibromatosis Type 2 (NF2) tumor suppressor, known as merlin and schwannomin (Sch) was identified as a plasma membrane-cytoskeleton linking protein based on its homology to the FERM family of proteins (Rouleau et al. 1993; Trofatter et al. 1993). SCs with inactivation of the *nf2* gene form benign slow growing schwannomas. When cultured, schwannoma cells do not assume the typical bipolar shape of SCs, but rather spread into large round flat cells with abundant ruffling membranes (Pelton et al. 1998). This altered morphology has been attributed at least in part to increased Rac, PAK and JNK activity which inhibits their ability to extend processes onto axons (Kaempchen et al. 2003; Nakai et al. 2006). Transgenic modification of *nf2* in mice perturbs peripheral nerve development (Giovannini et al. 2000; Denisenko et al. 2008). The abnormalities observed include axonal loss, aberrant myelination and disorganization of axoglial contacts. These results suggest that Sch plays a role in myelination, yet the mechanism(s) are unknown.

Sch regulates many signaling pathways initiated from multiple receptors to control proliferation, apoptosis and morphology (reviewed in Okada et al. 2007; Lallemand et al. 2009). A well-established mechanism by which Sch exercises its tumor suppressor function involves inhibition of Cdc42/Rac activation of p21-activated kinase (PAK) (Hirokawa et al. 2004; Kissil et al. 2003; Okada et al. 2005). This ability is inactivated by phosphorylation of Sch at serine 518 (S518) by protein kinase A (PKA) and Cdc42/Rac-PAK (Alfthan et al. 2004; Kissil et al. 2002; Xiao et al. 2002). We have demonstrated that activation of β1 integrin and erbB2 receptors promotes Sch-S518 phosphorylation in PAK and PKA dependent manners, respectively (Thaxton et al. 2008). Moreover, we found that β1 integrin and erbB2 receptors are enriched with Sch, Cdc42 and PAK at the distal tips of SC processes (Thaxton et al. 2008). These tips are highly motile structures similar to axonal growth cones and pathways initiated there mediate alignment and motility of SCs on axons (Gatto et al. 2003; Gatto et al. 2007). β1 integrin and erbB2 receptors transduce signals from the extracellular matrix and axons, respectively and are essential for SC function (Berti et al. 2006; Britsch 2007).

Sch also indirectly controls activation of Rac (Morrison et al. 2007) by controlling its translocation to the plasma membrane (Okada et al. 2005). Rac and Cdc42 GTPases have been reported to have essential but distinct roles during SC development (Feltri et al. 2008) but act synergistically in oligodendrocytes to regulate myelin sheath formation (Thurnherr et al. 2006). Sch is thus well-positioned to integrate signals from erbB2 and β1 integrin to

regulate Cdc42/Rac-dependent changes in SC morphology during peripheral nerve development.

2. MATERIALS AND METHODS

2.1. Materials

The human Sch-GFP, Sch-S518A-GFP, Sch-S518D-GFP constructs have been previously described (Thaxton et al. 2007). The Sch-BBA-GFP plasmid was constructed using *in vitro* mutagenesis. The following materials were used: mouse laminin, Lipofectamine 2000, Lipofectamine PLUS (Invitrogen, Carlsbad, CA), 2.5S nerve growth factor (NGF, Harlan, Indianapolis, IN). Antibodies were purchased from the following sources: Neurofilament H (Dako, Denmark), P-ERM (Cell Signaling, Davers, MA), PS518-Sch, Caspr and Cre (Abcam, Cambridge, MA), ErbB2 (EMD Biosciences, San Diego, CA), and Alexa Flour conjugated secondary antibodies (Invitrogen). All cell cultures reagents were purchased from Invitrogen.

2.2. Cell Culture and Transfection

2.2a. Preparation and Transfection of Rat SCs—Primary rat SCs were isolated from sciatic nerves of 1 day-old Sprague Dawley (Charles River, North Wilmington, MA) pups using the Brockes method (Brockes et al. 1979) with modifications described previously (Chen et al. 2000). Cells were plated on uncoated plastic dishes and were grown in DMEM with 10% fetal bovine serum (D10). Rapidly dividing fibroblasts were eliminated by growth in D10 containing 10^{-5} M cytosine arabinoside (Sigma-Aldrich, St. Louis, MO) for 5 days. Any remaining fibroblasts were eliminated by complement-mediated cell lysis using Thy 1.1 antibody (103-TIB, ATCC) and guinea pig complement (Rockland, Gilbertsville, PA). SCs were expanded on 200μg/ml poly-L-lysine (PLL, Sigma-Aldrich, St. Louis, MO) coated culture dishes in D10 supplemented with 2 μM forskolin (Sigma-Aldrich, St. Louis, MO) and 20 μg/ml pituitary extract (Biomedical Technologies, Stoughton, MA). Cultures were passaged no more than 6 times prior to use, and were only used if they were greater than 95% pure based on cellular morphology. For transfection experiments, purified SCs were plated on PLL (200 μg/ml) and laminin (25 μg/ml) coated German glass coverslips (Carolina Biol., Burlington, NC) and were transfected with GFP-tagged constructs using Lipofectamine 2000 as previously described (Thaxton et al., 2007). Immunostaining was carried out 36-48 hours later.

2.2b. Preparation and Transfection of Dissociated Rat DRGN/SC Co-cultures—Dorsal root ganglia (DRG) were harvested from Sprague Dawley rat embryos at 16 days of gestation (E16) and were dissociated as described previously (Chen et al. 2000). The equivalent of 1 DRG was seeded onto 12mm PLL (200μg/ml) and laminin (50μg/ml) coated German glass coverslips in EMEM, 5% FBS, 0.4% glucose, 50ηg/ml 2.5S NGF (CB5). One day after plating, DRG neuron (DRGN) cultures were pulsed for 3 days with anti-mitotic medium containing 10μM fluorodeoxyuridine (FdUr) in N2 medium containing 2.5S NGF to remove non-neuronal cells. Cultures were maintained in CB5 medium for one week to allow neurite extension. The dissociated DRGN cultures were seeded with primary rat SCs at 2×10^5 SCs per coverslip in EMEM, 10% FBS, 0.4% glucose, and 50ηg/ml 2.5S NGF (CB10) medium. Co-cultures were maintained in CB10 for 10-14 days until a high SC density was obtained. Co-cultures were then either transfected as described below, or were switched to M-feed (EMEM, 15% FBS, 0.4% glucose, 0.05mg/ml L-Ascorbic acid, 50ηg/ml 2.5S NGF) and were used in myelination time course studies. DRGN/SC co-cultures were transiently transfected with GFP-tagged constructs using Lipofectamine 2000 following the manufacturer's protocol. Briefly, co-cultures growing in CB10 were transfected with 250ηg of GFP-tagged constructs for 4 hours. After incubation, the culture medium was replaced

with fresh CB10. Twenty four hours after transfection, the medium was replaced with M-feed. The dissociated DRGN/SC co-cultures were fed every other day with M-feed for at least 10-12 days prior to fixation and immunostaining to assess myelination.

2.2c. Preparation and Transfection of Rat DRG Explant Cultures—DRG explants were cultured as previously described (Gatto et al. 2007; Howe and McCarthy, 1998). Briefly, spinal cords with associated DRGs were removed from E16 Wistar rat embryos (Charles River, North Wilmington, MA) and were rinsed in HBSS with calcium (1.2 mM), magnesium (0.8 mM), and supplemented with 5% FBS, 50 U/mL penicillin, and 50 μg/mL streptomycin. Ganglia were trimmed of spinal roots, removed from the cords, rinsed with HBSS without serum and were grown in Basal Eagle's Medium (BME) including ITS+ supplements, 0.2% BSA, 10 mM HEPES, 498 mg/dL D-glucose, 100ηg/mL 2.5S NGF, 50 U/mL penicillin, and 50 μg/mL streptomycin on glass coverslips coated with 0.4 mg/mL Matrigel in BME and 10 μg/mL poly-D-lysine placed on Teflon circles. 21 day-old DRG explant cultures were transfected using Lipofectamine PLUS (Pedraza and Colman, 2000). One microgram of DNA/coverslip was used and the DNA/PLUS (3.5 μL)/Lipofectamine (2.8 μL) complexes were incubated with the cultures for 3-4 hours in unsupplemented BME. The transfection mixture was then removed. The cultures were rinsed once with BME and were returned to the supplemented BME medium.

2.3. Generation of Mouse *nf2$^{flox2/flox2}$* SCs and Cre-Mediated Inactivation

The *nf2$^{flox2/flsox2}$* mice were obtained from Dr. Marco Giovannini (Giovannini et al 2000; HEI, Los Angeles, CA). Sciatic nerves were harvested from adult homozygous floxed mice, and SCs were isolated using the method published by Pannunzio et al (2005). Briefly, sciatic nerves from 6 to 8 week old mice were digested with dispase and collagenase and were plated in N2 medium containing N2 Supplement, 2 μM forskolin (Sigma-Aldrich, St. Louis, MO) and 10ng/ml glial growth factor (generous gift from Dr. M. Marchionni). SCs were infected with *adeno-Cre* or *adeno-LacZ* viruses (University of Iowa Gene Transfer Vector Core) at 200–400 multiplicity of infection. SCs were immunostained with Cre, β-galactosidase and erbB2 antibodies 2-10 days after infection.

2.4. Immunostaining and Live Cell Imaging

Primary rat SC cultures were fixed with 4% paraformaldehyde, washed with phosphate buffer, immunostained with antibodies and mounted in Gel Mount (BioMeda, CA, USA). Immunostaining for the DRGN/SC neuron co-cultures was described previously (Thaxton et al. 2007). All cultures were analyzed with a Zeiss laser scanning microscope and LSM510 software. Images are single planes and were processed identically. Live cell imaging of transfected DRG explants was carried out as previously described (Gatto et al. 2007). Co-transfected cultures were immunostained *in situ* with antibodies to the HA epitope and Sch after live cell imaging to ensure that imaged cells expressed both GFP and HA variants.

2.5. Statistical Analysis

For quantification of process length, three independent transfection experiments were carried out using the indicated plasmids. The lengths of approximately 60-70 cellular processes from each condition per experiment were measured. Statistical significance (p-value) was obtained using a standard unpaired t-test (GraphPad Software, Inc., La Jolla, CA). For quantification of SC length in DRG explants co-transfected with Sch-GFP and Rac variants, two coverslips for each of the transfection combinations from three independent transfection experiments were evaluated. The lengths of approximately 40-50 cells per coverslip were measured and the statistical significance (p-value) between different pairs of transfection/co-transfection conditions was calculated using a paired t-test. For

quantification of myelin length, four experiments were conducted and all GFP-labelled myelin segments were measured. Myelin was identified by MAG immunoreactivity, Caspr localization, and confirmed by morphology using phase and differential interference contrast optics (DIC). The distribution of lengths and the mean and SEM of all segments observed in the experiments are shown. Significance was calculated using unpaired t-test. The mean fold change was calculated from two experiments with equivalent transfection and myelination efficiencies. For all other experiments, a minimum of three repetitions was conducted and representative results are shown.

3. RESULTS

3.1. Sch Promotes Elongation of Bipolar Processes in Isolated SCs

To assess Sch's role in regulating SC morphology, we transiently transfected primary rat SCs with GFP, Sch-GFP, and the dominant negative variant, Sch-BBA-GFP (LaJeunesse et al. 1998; Johnson et al. 2002), and compared cell shape and process length (Figure 1A-C, Table 1). SCs expressing GFP alone were typically bipolar, similar to normal confluent SCs. The lengths of their processes ranged from 21μm to 520μm, with the highest percentage of processes falling between 51-100 μm. On average, GFP-expressing processes measured 140±6μm. Sch-GFP-expressing SCs were similarly bipolar in shape, but their process lengths were significantly increased with a mean of 256±11μm (p-value ≤ 0.0001) compared to GFP-expressing SCs. This represents an 82% increase in length compared to GFP-expressing SCs. Moreover, the process lengths of Sch-GFP-expressing SCs ranged between 30μm to 951μm, with the most frequent range falling between 151-200μm. In contrast, SCs expressing Sch-BBA-GFP, a dominant negative form that perturbs the function of endogenous Sch, elaborated processes between 28μm and 380μm in length. The highest percentage of Sch-BBA-GFP processes fell between 51-100 μm. The mean length was 118±5 μm, a 15% decrease compared to GFP-expressing SCs ($p<0.005$) and a 64% decrease compared to Sch-GFP-expressing ($p<0.0001$) SCs. Notably, approximately 15% of the population of Sch-GFP-expressing SCs extended processes longer than 401μm. In contrast, less than 5% of GFP-expressing SCs and none of the Sch-BBA-GFP-expressing SCs extended processes longer than 401μm. Together, these results indicate that Sch promotes elongation of bipolar cellular processes in SCs.

Next we sought to determine whether Sch was necessary for maintenance of the SC bipolar morphology. For this experiment, purified mouse SCs isolated from sciatic nerves of $nf2^{flox2/flox2}$ mice (Giovannini et al. 2000) were infected with Ad-Cre virus to cause an in-frame deletion of exon 2 (amino acids 39-80). Subsequently expressed Sch lacks a paxillin binding domain (amino acids 50-70) required for plasma membrane localization and serine 518 phosphorylation, and degrades more rapidly than full-length Sch (Fernandez-Valle et al. 2002; Thaxton et al. 2007; unpublished data). *Ad-Cre* and control Ad-*LacZ* infected $nf2^{flox2/flox2}$ mouse SCs were immunostained with antibodies to Cre, β-galactosidase and ErbB2 to visualize the cells. The *Ad-Cre* SCs transitioned to a multipolar phenotype within 5-9 days of infection. This result was consistently observed in approximately 20 experiments conducted over several years (Figure 1D). In contrast, the βGal-expressing SCs remained bipolar and extended long processes, thus ruling out non-specific effects of viral infection. This result demonstrates that Sch function is required for SCs to assume and/or maintain their characteristic bipolar morphology.

3.2. Sch Facilitates SC Alignment on Axons

To test whether Sch promoted the extension of bipolar processes in SCs interacting with axons, we transiently transfected embryonic rat DRG explant cultures with Sch-GFP and Sch-BBA-GFP constructs and quantified the number of GFP-positives processes emanating

from the SC body. Sch-GFP-expressing SCs were predominantly bipolar and tripolar; 40% and 42% of total transfected SCs, respectively. In contrast, 50% of Sch-BBA-GFP-expressing SCs were multipolar, with more than three processes extending from the cell body (Figure 2A-B). The increase in multipolar SCs arose from the loss of bipolar SCs from the population. Only 10% of the Sch-BBA-GFP-expressing SCs were bipolar in contrast to 40% of Sch-GFP-expressing SCs. We conclude that Sch functions similarly in axon-associated and isolated SCs; it induces a bipolar phenotype and/or is necessary for its maintenance.

To assess whether Sch promoted the interaction of SCs with axons, we transiently transfected 5 day-old rat DRG cultures with GFP and Sch-GFP plasmids and examined their association over time. Previously, we demonstrated that satellite SCs migrated from DRG explants concomitant with neurite extension (Gatto et al. 2003). Initially, cells exhibited a flattened fibroblastic morphology but over the ensuing 10-12 days, they aligned on axons and adopted a bipolar morphology. Here we found that Sch-GFP-expressing SCs had already contacted and elongated along axons five days after transfection (Figure 2C). At this same time point, control GFP-expressing SCs still adhered to the substrate and displayed a fibroblastic morphology. This result is consistent with the conclusion that Sch facilitates axon-directed process extension and alignment of SCs with axons *in vitro*.

3.3. Sch Regulates SC Morphology and Process Length by Inhibiting Rac Activity

Sch has been shown to indirectly inhibit Rac and Ras GTPase activity (Morrison et al., 2008). Furthermore, SCs with conditional inactivation of *Rac-1* are unable to extend processes and carry out radial sorting of axons *in vivo* (Beninger et al. 2007; Nodari et al 2007). To determine whether Sch's effect on process elongation involved regulation of Rac activity, we transiently co-transfected DRG explant cultures with plasmids encoding GFP and Sch-GFP, as well as HA-tagged dominant negative (RacN17) and constitutively active (RacV12) forms of Rac. The transfected SCs were immunostained with antibodies against the HA tag, and the entire length of GFP- and HA-positive SCs was measured and compared (Figure 3). The mean length of axon-aligned GFP-expressing SCs was 189±11μm, whereas the mean lengths of Sch-GFP and RacN17 expressing SCs were 266±13μm and 228±16μm, respectively. These represented a 41% and 21% increase in SC length compared to GFP-expressing SCs ($p<0.0001$). The expression of GFP alone did not affect SC length as SCs expressing GFP and RacN17, or RacN17 alone yielded statistically indistinguishable SC lengths (data not shown). Co-expression of Sch-GFP with RacN17 (254±14μm) did not promote a statistically significant increase in SC length compared to those expressing Sch-GFP (266±13μm) or RacN17 (228±16μm) alone. In contrast, the mean length of RacV12-expressing SCs was 149±5μm, a 21% reduction compared to GFP-expressing SCs. Conversely, SCs co-expressing Sch-GFP and RacV12 had a mean length of 225±12μm, a 15% reduction in overall length compared to Sch-GFP expressing SCs. This result indicates that suppression of Rac activity promotes bipolar elongation of SCs and suggests that Sch promotes SC elongation by inhibiting Rac-dependent signals.

To further investigate the effect of Sch and Rac expression on SC dynamics, we carried out live imaging of DRG explant cultures transfected with the HA-Rac variants and untagged Sch and GFP plasmids. 36 hours after transfection, the GFP-expressing SCs were imaged for 18 hours and then were immunostained with antibodies against the HA epitope and Sch to ensure co-transfection with GFP plasmids (Figure 4). SCs co-expressing HA-RacV12 and GFP were highly dynamic and motile and transitioned between unipolar, bipolar and multipolar morphologies but did not align on axons (Figure 4; compare t=0, t=60 and t=600 minute time points in RacV12, and Supplementary Movie 1). In contrast, SCs co-expressing HA-RacN17 and GFP were markedly less dynamic over the same time period compared to SCs expressing RacV12 (Supplementary Movie 2). These SCs remained bipolar, slowly

elongated processes, or transitioned into unipolar cells and migrated along axons. SCs expressing Sch, although overall more dynamic, behaved similarly to those expressing Rac N17; slowly elongating processes to become bipolar cells during the period of observation (Supplementary Movie 3). Together, these results suggests that a mechanism by which Sch specifies the bipolar shape of SCs is by inhibiting Rac-dependent pathways that promote plasma membrane and cytoskeletal remodeling.

3.4. SCs Expressing Sch-GFP Form Atypically Long Myelin Internodes

Factors and mechanisms that regulate the myelin segment length are largely unknown. Because over-expression of Sch resulted in longer SCs, we hypothesized that this increase in length would translate into an increase in myelin segment length. To test this, we used dissociated embryonic rat DRGN co-cultured with purified neonatal rat SCs. This preparation eliminates fibroblasts and leads to more reliable myelination. DRGN/SC co-cultures were transiently transfected with plasmids encoding GFP, Sch-GFP, and Sch-BBA-GFP twenty-four hours prior to adding M-feed to initiate SC differentiation. 10-12 days later, the internodal length of GFP-positive myelin segments was measured (Figure 5A-C). (Myelin was identified by MAG and Caspr expression and light microscopy; not shown). GFP-positive myelin segments ranged in length between 56-237μm with the highest frequency (30%) occurring at 101-125μm, and had a mean of 127±3μm. The mean length of Sch-GFP-positive myelin segments was 147±3μm, a statistically significantly 16% increase over GFP controls ($p<0.0001$). They ranged in length between 96-240 μm with the highest frequency (28%) at 126-150μm. Notably, myelin segments were not observed in co-cultures transfected with Sch-BBA-GFP plasmids (data not shown). These SCs did not align with axons and assumed a multipolar morphology similar to Sch-BBA-GFP expressing SCs in DRG explant cultures (Figure 2). We concluded that Sch-BBA-GFP-expressing SCs did not myelinate because they were unable to stably align on axons as bipolar cells.

Sch transitions between a serine 518 phosphorylated, open conformation and a serine 518 unphosphorylated, closed conformation. The unphosphorylated, closed conformation functions as a tumor suppressor and inhibits Rac activity, while the phosphorylated form lacks tumor suppressor activity (Surace et al. 2004). To investigate whether the phosphorylation state of Sch-S518 affected the myelin segment length, we transiently transfected DRGN/SC co-cultures with plasmids encoding Sch-S518A-GFP, which mimics unphosphorylated Sch, and Sch-S518D-GFP, which mimics phosphorylated Sch. The experiment was carried out as described above. The mean lengths of Sch-S518A-GFP and Sch-S518D-GFP myelin segments were 157±3.7μm and 160±5μm, respectively and were not statistically different. Together, these results demonstrate that over-expression of Sch increases myelin length by a mechanism independent of S518 phosphorylation.

We also quantified the number of GFP-positive myelinating SCs in the DRGN/SC co-cultures. Experiments exhibiting equivalent transfection and myelination efficiencies were compared (Figure 5D). The mean number of myelin segments formed by GFP-expressing SCs was 21±6 per co-culture and while low, this value was consistently observed. The mean number of myelin segments formed by Sch-GFP-expressing SCs was 35±16 per co-culture, a 1.57-fold increase compared to GFP controls. An additional increase to 41±11 GFP-labelled myelin segments per co-culture was observed when Sch-S518A-GFP was expressed. This was nearly a 2-fold increase compared to GFP controls. In contrast, there was a statistically significant 20% decrease in the number of myelinating SCs in co-cultures transfected with Sch-S518D-GFP compared to GFP alone (17±5 vs. 21±6) and a 60% reduction compared to co-cultures transfected with Sch-S518A-GFP, (17±5 vs. 41±11). This result suggests that Sch-S518 phosphorylation plays a role in promoting differentiation of SCs into myelinating cells.

3.5 Sch Expression Does Not Affect Paranodal and Nodal Organization

Recently, a role for Sch in regulating axo-glial interactions was reported in mice with conditional inactivation of *nf2* (Denisenko et al. 2008). In order to assess whether the increased internodal length was due to aberrant formation of axo-glial contacts, we immunostained the transfected co-cultures with antibodies against Caspr, a paranodal marker (Einheber et al. 1997) and phosphorylated ezrin (P-ERM), a marker for the SC nodal microvilli compartment (Gatto et al. 2003). Caspr localized normally in SCs expressing GFP, Sch-GFP, Sch-S518A-GFP, and Sch-S518D-GFP (Figure 6). Only a few myelinating SCs expressing Sch-S518D-GFP had slightly altered Caspr localization (Figure 6). This was attributed to the differences in the localization of GFP versus Sch-GFP rather than to changes in the sub-cellular myelin architecture. P-ERM localized normally to the distal-most nodal regions of myelinating SCs expressing GFP, Sch-GFP, Sch-S518A-GFP, and Sch-S518D-GFP. These results suggest that the Sch-mediated increase in the myelin internodal length was not associated with perturbations in the paranodal and nodal compartments as revealed by these markers.

4. DISCUSSION

The major findings of this study are that 1) Sch is essential for SCs to assume and maintain the bipolar spindle morphology and stably align with axons, and 2) the mechanism by which Sch promotes cellular elongation likely involves its ability to inhibit Rac-dependent signaling. We conclude that Sch-dependent temporal inhibition of Rac activity is necessary for final elongation of SCs on axons prior to myelination.

4.1. Sch Promotes Bipolar Elongation of Isolated and Axon-associated SCs

Over-expression of Sch in purified neonatal rat SCs stimulated elongation of bipolar processes creating SCs dramatically longer than those expressing GFP alone. The longest Sch-GFP-expressing SCs were over 1mm in length. In contrast, over-expression of dominant-negative Sch-BBA inhibited process elongation and resulted in significantly shorter SCs compared to GFP-expressing controls. Interestingly, when introduced into SCs growing with neurons, the Sch-BBA construct caused the SCs to become multipolar, a morphology that was incompatible with axon alignment and myelination. The BBA form of Sch has alanines substituting the seven amino acid domain termed the “blue box” (BB) found in the FERM domain. Deletion or substitution of the BB domain creates a dominant negative form of *Drosophila* merlin (Sch) that localizes exclusively to the plasma membrane but cannot limit cell proliferation, and blocks activity of endogenous Sch (LaJeunesse et al. 1998). Expression of Sch-BBA in 3T3 fibroblasts reduces F-actin stress fibers and causes their transformation (Johnson et al. 2002). These observations indicate that actin dynamics is regulated by plasma membrane associated as opposed to intracellular Sch. Here we demonstrated that deletion of *nf2* exon 2 that encodes the plasma membrane targeting domain in Sch resulted in formation of multipolar SCs. Overall, these results indicate that plasma-membrane associated Sch promotes the bipolar morphology and regulates SC length.

4.2. Sch Inhibits Rac Signaling to Promote Bipolar Process Formation and SC Elongation

Sch has the ability to act both upstream and downstream of Rac to regulate Rac-dependent signaling. Sch functions upstream of Rac by inhibiting its recruitment to the plasma membrane where it is activated by receptor dependent mechanisms (Okada et al. 2005; Del Pozo and Schwartz, 2007; Morrison et al. 2007). Sch functions downstream of Rac by directly binding to Pak’s CRIB (Cdc42/Rac interactive binding) thereby preventing its activation (Kissil et al. 2003). In this study, we observed evidence for both mechanisms. Over-expression of dominant-negative Rac induced an elongated stable phenotype comparable to that observed in SCs over-expressing Sch. Importantly, this reveals that the

bipolar phenotype arises when Rac activity is reduced. Moreover, the elongation associated with Sch over-expression was partially overcome by co-expression of constitutively active RacV12. This result supports the conclusion that Sch acts upstream of Rac to inhibit Rac-dependent signaling. The inability of RacV12 to completely inhibit Sch-induced elongation supports the conclusion that Sch also acts downstream to directly inhibit Rac effectors such as Pak. Other possible interpretations are that Rac-independent mechanisms are involved or simply that unequal amounts of the respective plasmids were introduced into individual SCs.

Figure 7 summarizes our findings. Overexpression of Sch results in an elongated SC that gives rise to an elongated myelin segment. In contrast, perturbation of endogenous Sch function using the dominant-negative BBA mutant results in a multipolar cell unable to align with axons and hence myelinate. This idea is supported by the observation that schwannoma cells from NF2 patients exhibit high Rac activity and are unable to align with axons unless treated with Rac inhibitors (Pelton et al. 1998; Nakai et al. 2006). A potential mechanism by which Sch-dependent inhibition of Rac activity could lead to cellular elongation is through suppression of axial process retraction concomitant with suppression of new process growth from the cell body. This would be consistent with morphological effects of Rac activity in other cell types. For example, Rac activity has been shown to promote the formation of peripheral lamellae in fibroblasts and epithelial cells to mediate random-directed motility (Pankov et al, 2005). Intriguingly, these cell types adopt the bipolar spindle morphology when Rac activity is inhibited. Our findings support the idea that Sch promotes the bipolar SC morphology by suppressing Rac activation at the plasma membrane.

4.3. Receptor Mediated Phosphorylation of Sch and Potential Role During Peripheral Nerve Development and Myelination

Our results indicate that suppression of Rac activity is required for SCs to maintain a bipolar phenotype and align with axons just prior to active myelination. However, Rac activity is required during axon sorting, an earlier stage of development (Beninger et al. 2007; Nodari et al, 2007). We propose that spatial-temporal regulation of Sch phosphorylation on S518 could be used to modulate Rac activity in response to ErbB2 and β1 integrin activation during key stages of myelination. We previously demonstrated that Sch through a direct interaction with paxillin localizes to the plasma membrane and associates with ErbB2 and β1 integrin (Fernandez-Valle et al. 2002; Obremski et al. 1998), receptors that provide signals crucial for initiation of myelination. NRG and laminin, ligands for these receptors stimulate PKA and Cdc42/PAK-dependent phosphorylation of Sch on S518, respectively, in SCs (Thaxton et al. 2008). We propose that SCs with high levels of S518 phosphorylated Sch would be multipolar, a phenotype necessary for the radial sorting stage. In support of this model, we have shown that isolated SCs expressing the phospho-mimetic (S518D) variant of Sch are predominantly multipolar (Thaxton et al. 2007). Here we demonstrated that they are compromised in their ability to myelinate likely because they cannot transition into axon-aligned bipolar SCs. This raises the possibility that similar to the Sch-BBA-GFP-expressing SCs, SCs expressing Sch S518D-GFP were unable to assume a 1:1 association with axons, and receive signals that trigger differentiation into myelinating cells. Alternatively, SCs expressing Sch-S518D-GFP could be unable to exit the cell cycle and differentiate because this form lacks tumor suppressor function.

We propose that the levels of S518 phosphorylated Sch gradually decline as radial sorting is completed allowing SCs to transition into bipolar SCs and establish a stable 1:1 association with axons. Polarization of ErbB2 receptors to the adaxonal membrane could trigger PKA dependent phosphorylation of Sch along the inner mesaxon stimulating a burst of Rac activity needed for expansion of the plasma membrane during active myelination.

Finally, the length of the myelin internode is closely correlated with axon diameter to allow for effective saltatory conduction (Rushton 1951). However, signals and factors that regulate the myelin internode length are relatively unknown. The *nf2* gene has been conditionally inactivated in mice using a P0 promoter driven Cre and resulted in shortened myelin internodes (Denisenko et al. 2008). It was hypothesized that increased SC number accounted for the shortened myelin segments. However, our *in vitro* results offer an alternative explanation, i.e., that SCs lacking Sch were compromised in their ability to extend bipolar processes and fully elongate on axons. We demonstrated that simply altering the pre-myelinating length of the SC by overexpressing Sch increased the internodal length. It would be of interest to determine whether this increase correlates with an increase in the axonal diameter.

In summary, we provide evidence for a role of Sch in promoting SC elongation and alignment on axons as bipolar cells. Sch appears to function at least in part by inhibiting Rac activity and/or Rac-dependent signaling to restrict formation of perpendicular processes and promote elongation of axial processes. This restricted growth pattern facilitates SC alignment on axons and influences the final myelin segment length *in vitro*.

Supplementary Material

Refer to Web version on PubMed Central for supplementary material.

Acknowledgments

We thank M Giovannini for the $nf2^{flox2/flox2}$ mouse, M. Marchionni for the generous gift of recombinant glial growth factor, and Caroline Thompson, Teresa Kritsch and Robert Banks for animal husbandry. This work was supported by CDMRP/NFRP award DAMD 17-02-1-0649 and NIH award RO1-DC010189 to CFV and CDMRP/NFRP award W81X-WH-06-1-0216 to SL. This work is dedicated to the memory of Barbara Walker.

Abbreviations

SC	Schwann cell
NF2	Neurofibromatosis Type 2
PAK	p21-activated kinase
PKA	protein kinase A
DRG	dorsal root ganglion
NGF	nerve growth factor
NRG	neuregulin beta-1

References

Alfthan K, Heiska L, Gronholm M, Renkema GH, Carpen O. Cyclic AMP-dependent protein kinase phosphorylates merlin at serine 518 independently of p21-activated kinase and promotes merlin-ezrin heterodimerization. J Biol Chem. 2004; 279(18):18559–66. [PubMed: 14981079]

Benninger Y, Thurnherr T, Pereira JA, Krause S, Wu X, Chrostek-Grashoff A, Herzog D, Nave KA, Franklin RJ, Meijer D. Essential and distinct roles for cdc42 and rac1 in the regulation of Schwann cell biology during peripheral nervous system development. J Cell Biol. 2007; 177(6):1051–61. [PubMed: 17576798]

Berti C, Nodari A, Wrabetz L, Feltri ML. Role of integrins in peripheral nerves and hereditary neuropathies. Neuromolecular Med. 2006; 8(1-2):191–204. [PubMed: 16775376]

Britsch S. The neuregulin-I/ErbB signaling system in development and disease. Adv Anat Embryol Cell Biol. 2007; 190:1–65. [PubMed: 17432114]

Brockes JP, Fields KL, Raff MC. Studies on cultured rat Schwann cells. I. Establishment of purified populations from cultures of peripheral nerve. Brain Res. 1979; 165(1):105–18. [PubMed: 371755]

Chen LM, Bailey D, Fernandez-Valle C. Association of beta 1 integrin with focal adhesion kinase and paxillin in differentiating Schwann cells. J Neurosci. 2000; 20(10):3776–84. [PubMed: 10804218]

Del Pozo MA, Schwartz MA. Rac, membrane heterogeneity, caveolin and regulation of growth by integrins. Trends Cell Biol. 2007; 17(5):246–50. J Neurosci. 2008 Oct 15;28(42):10472-81. [PubMed: 17363257]

Denisenko N, Cifuentes-Diaz C, Irinopoulou T, Carnaud M, Benoit E, Niwa-Kawakita M, Chareyre F, Giovannini M, Girault JA, Goutebroze L. Tumor suppressor schwannomin/merlin is critical for the organization of Schwann cell contacts in peripheral nerves. J Neurosci. 2008; 28(42):10472–81. [PubMed: 18923024]

Einheber S, Zanazzi G, Ching W, Scherer S, Milner TA, Peles E, Salzer JL. The axonal membrane protein Caspr, a homologue of neurexin IV, is a component of the septate-like paranodal junctions that assemble during myelination. J Cell Biol. 1997; 139(6):1495–506. [PubMed: 9396755]

Feltri ML, Suter U, Relvas JB. The Function of RhoGTPases in Axon Ensheathment and Myelination. Glia. 2008; 56:1508–17. [PubMed: 18803320]

Fernandez-Valle C, Tang Y, Ricard J, Rodenas-Ruano A, Taylor A, Hackler E, Biggerstaff J, Iacovelli J. Paxillin binds schwannomin and regulates its density dependent localization and effect on cell morphology. Nat Genet. 2002; 31(4):354–62. [PubMed: 12118253]

Gatto CL, Walker BJ, Lambert S. Local ERM activation and dynamic growth cones at Schwann cell tips implicated in efficient formation of nodes of Ranvier. J Cell Biol. 2003; 162(3):489–98. [PubMed: 12900397]

Gatto CL, Walker BJ, Lambert S. Asymmetric ERM activation at the Schwann cell process tip is required in axon-associated motility. J Cell Physiol. 2007; 210(1):122–32. [PubMed: 17061246]

Giovannini M, Robanus-Maandag E, van der Valk M, Niwa-Kawakita M, Abramowski V, Goutebroze L, Woodruff JM, Berns A, Thomas G. Conditional biallelic Nf2 mutation in the mouse promotes manifestations of human neurofibromatosis type 2. Genes Dev. 2000; 14(13):1617–30. [PubMed: 10887156]

Hirokawa Y, Tikoo A, Huynh J, Utermark T, Hanemann CO, Giovannini M, Xiao GH, Testa JR, Wood J, Maruta H. A clue to the therapy of neurofibromatosis type 2: NF2/merlin is a PAK1 inhibitor. Cancer J. 2004; 10(1):20–6. [PubMed: 15000491]

Howe DG, McCarthy KD. A dicistronic retroviral vector and culture model for analysis of neuron-Schwann cell interactions. J Neurosci Methods. 1998; 83(2):133–42. [PubMed: 9765126]

Johnson KC, Kissil JL, Fry JL, Jacks T. Cellular transformation by a FERM domain mutant of the Nf2 tumor suppressor gene. Oncogene. 2002; 1(39):5990–7. [PubMed: 12203111]

Kaempchen K, Mielke K, Utermark T, Langmesser S, Hanemann CO. Upregulation of the Rac1/JNK signaling pathway in primary human schwannoma cells. Hum Mol Genet. 2003; 12(11):1211–21. [PubMed: 12761036]

Kissil JL, Johnson KC, Eckman MS, Jacks T. Merlin phosphorylation by p21-activated kinase 2 and effects of phosphorylation on merlin localization. J Biol Chem. 2002; 277(12):10394–9. [PubMed: 11782491]

Kissil JL, Wilker EW, Johnson KC, Eckman MS, Yaffe MB, Jacks T. Merlin, the product of the Nf2 tumor suppressor gene, is an inhibitor of the p21-activated kinase, Pak1. Mol Cell. 2003; 12(4): 841–9. [PubMed: 14580336]

LaJeunesse DR, McCartney BM, Fehon RG. Structural analysis of Drosophila merlin reveals functional domains important for growth control and subcellular localization. J Cell Biol. 1998; 141(7):1589–99. [PubMed: 9647651]

Lallemand D, Manent J, Couvelard A, Watilliaux A, Siena M, Chareyre F, Lampin A, Niwa-Kawakita M, Kalamarides M, Giovannini M. Merlin regulates transmembrane receptor accumulation and signaling at the plasma membrane in primary mouse Schwann cells and in human schwannomas. Oncogene. 2009; 28(6):854–65. [PubMed: 19029950]

Lappe-Siefke C, Goebbels S, Gravel M, Nicksch E, Lee J, Braun PE, Griffiths IR, Nave KA. Disruption of Cnp1 uncouples oligodendroglial functions in axonal support and myelination. Nat Genet. 2003; 33(3):366–74. [PubMed: 12590258]

Morrison H, Sperka T, Manent J, Giovannini M, Ponta H, Herrlich P. Merlin/neurofibromatosis type 2 suppresses growth by inhibiting the activation of Ras and Rac. Cancer Res. 2007; 67(2):520–7. [PubMed: 17234759]

Nakai Y, Zheng Y, MacCollin M, Ratner N. Temporal control of Rac in Schwann cell-axon interaction is disrupted in NF2-mutant schwannoma cells. J Neurosci. 2006; 26(13):3390–5. [PubMed: 16571745]

Nodari A, Zambroni D, Quattrini A, Court FA, D'Urso A, Recchia A, Tybulewicz VL, Wrabetz L, Feltri ML. Beta1 integrin activates Rac1 in Schwann cells to generate radial lamellae during axonal sorting and myelination. J Cell Biol. 2007; 177(6):1063–75. [PubMed: 17576799]

Obremski VJ, Hall AM, Fernandez-Valle C. Merlin, the neurofibromatosis type 2 gene product, and beta1 integrin associate in isolated and differentiating Schwann cells. J Neurobiol. 1998; 37(4): 487–501. [PubMed: 9858254]

Okada T, Lopez-Lago M, Giancotti FG. Merlin/NF-2 mediates contact inhibition of growth by suppressing recruitment of Rac to the plasma membrane. J Cell Biol. 2005; 171(2):361–71. [PubMed: 16247032]

Okada T, You L, Giancotti FG. Shedding Light on Merlin's Wizadry. Trend Cell Biol. 2007; 17(5): 222–229.

Pankov R, Endo Y, Even-Ram S, Araki M, Clark K, Cukierman E, Matsumoto K, Yamada KM. A Rac switch regulates random versus directionally persistent cell migration. J Cell Biol. 2005; 170(5): 793–802. [PubMed: 16129786]

Pedraza L, Colman DR. Fluorescent myelin proteins provide new tools to study the myelination process. J Neurosci Res. 2000; 60(6):697–703. [PubMed: 10861781]

Pelton PD, Sherman LS, Rizvi TA, Marchionni MA, Wood P, Friedman RA, Ratner N. Ruffling membrane, stress fiber, cell spreading and proliferation abnormalities in human Schwannoma cells. Oncogene. 1998; 17(17):2195–209. [PubMed: 9811451]

Pannunzio ME, Jou IM, Long A, Wind TC, Beck G, Balian G. A New Method of Selecting Schwann Cells from Adult Mouse Sciatic Nerve. J Neurosci Methods. 2005; 149(1):74–81. [PubMed: 15970332]

Rouleau GA, Merel P, Lutchman M, Sanson M, Zucman J, Marineau C, Hoang-Xuan K, Demczuk S, Desmaze C, Plougastel B. Alteration in a new gene encoding a putative membrane-organizing protein causes neuro-fibromatosis type 2. Nature. 1993; 363(6429):515–21. [PubMed: 8379998]

Rushton WAH. A Theory of the Effects of Fibre Size in Medullated Nerve. J Physiol (Lond). 1951; 115:101–122. [PubMed: 14889433]

Surace EI, Haipek CA, Gutmann DH. Effect of merlin phosphorylation on neurofibromatosis 2 (NF2) gene function. Oncogene. 2004; 23(2):580–7. [PubMed: 14724586]

Thaxton C, Lopera J, Bott M, Baldwin ME, Kalidas P, Fernandez-Valle C. Phosphorylation of the NF2 tumor suppressor in Schwann cells is mediated by Cdc42-Pak and requires paxillin binding. Mol Cell Neurosci. 2007; 34(2):231–42. [PubMed: 17175165]

Thaxton C, Lopera J, Bott M, Fernandez-Valle C. Neuregulin and laminin stimulate phosphorylation of the NF2 tumor suppressor in Schwann cells by distinct protein kinase A and p21-activated kinase-dependent pathways. Oncogene. 2008; 27(19):2705–15. [PubMed: 17998937]

Thurnherr T, Benninger Y, Wu X, Chrostek A, Krause SM, Nave KA, Franklin RJ, Brakebusch C, Suter U, Relvas JB. Cdc42 and Rac1 signaling are both required for and act synergistically in the correct formation of myelin sheaths in the CNS. J Neurosci. 2006; 26(40):10110–9. [PubMed: 17021167]

Trofatter JA, MacCollin MM, Rutter JL, Murrell JR, Duyao MP, Parry DM, Eldridge R, Kley N, Menon AG, Pulaski K. A novel moesin-, ezrin-, radixin-like gene is a candidate for the neurofibromatosis 2 tumor suppressor. Cell. 1993; 72(5):791–800. [PubMed: 8453669]

Xiao GH, Beeser A, Chernoff J, Testa JR. p21-activated kinase links Rac/Cdc42 signaling to merlin. J Biol Chem. 2002; 277(2):883–6. [PubMed: 11719502]

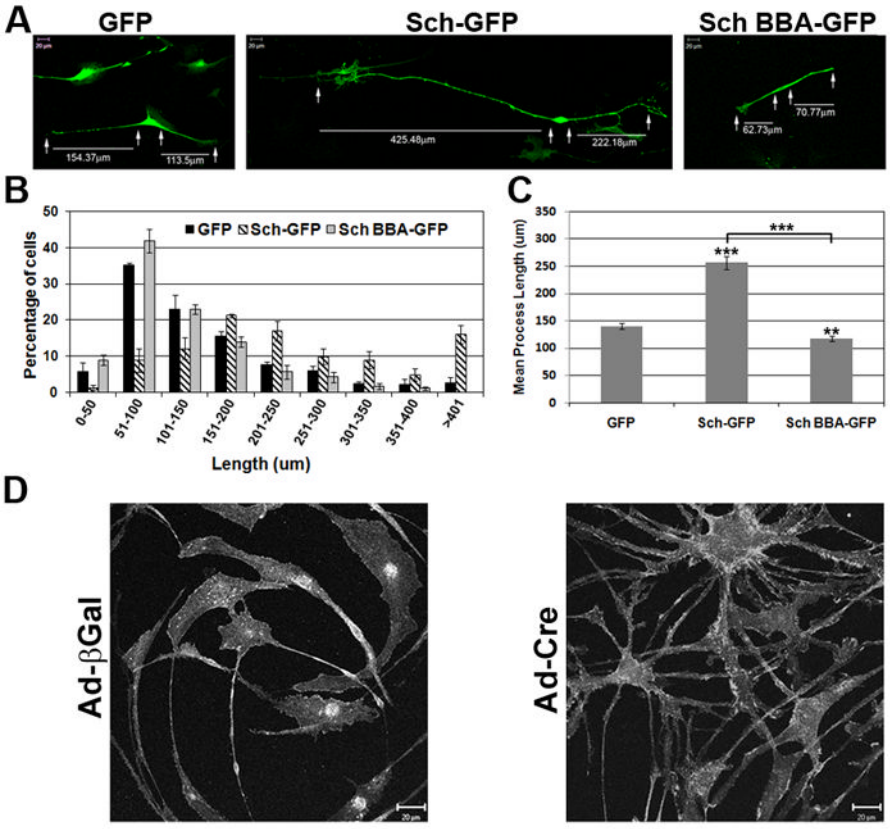

Figure 1. Sch Promotes Bipolar Elongation and Maintenance in Isolated Rat SCs

(A) Purified neonatal rat SCs were transiently transfected with GFP, Sch-GFP and Sch BBA-GFP in three experiments. GFP fluorescence was imaged three days after transfection. The length of each bipolar process was measured (arrows). Scale bars indicate 20μm. (B) The frequency histogram represents the mean percent and SEM of processes within the indicated range of the 3 experiments. (C) The mean process length shown is the mean of all processes measured over 3 experiments. The error bar represents the standard error of the mean (SEM). GFP (n= 227), Sch-GFP (n=183), and Sch BBA-GFP (n= 203). Asterisks denote statistical significance with p-values as follow: (*) ≤0.05, (**) ≤0.005, (***) ≤ 0.0001. (D) *Nf2*$^{flox2/flox2}$ adult mouse SCs were infected with an adenovirus directing expression of β-galactosidase (*Ad-βgal*) or Cre recombinase (*Ad-Cre*). Nine days after infection, SCs were immunostained for erbB2 receptors to visualize cells. SCs expressing Cre become multipolar, whereas those expressing β-galactosidase remain bipolar.

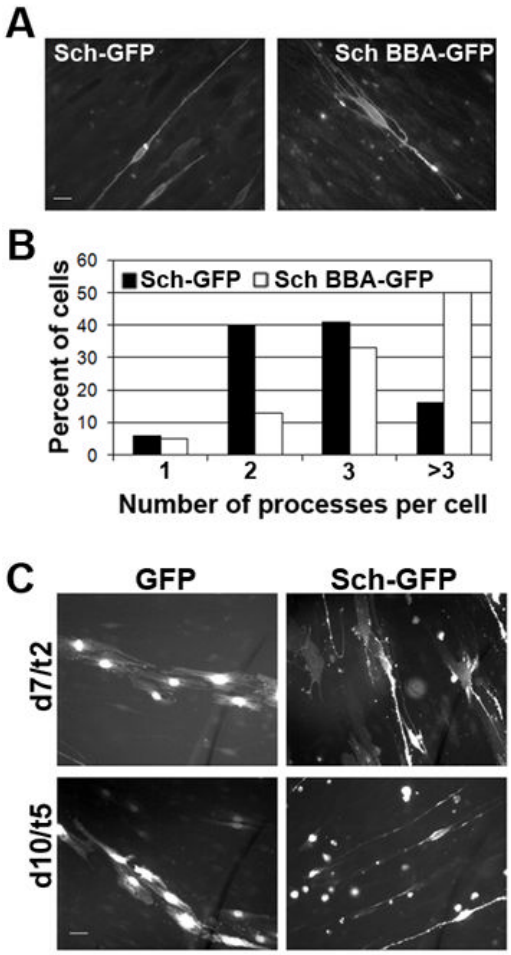

Figure 2. Sch Promotes Acquisition of the Bipolar Morphology and Alignment on Axons

(A) 21 day-old embryonic rat DRG explants cultures were transiently transfected with Sch-GFP and dominant negative Sch-BBA-GFP. (B) The morphology of GFP expressing SCs was assessed by counting the number of processes emanating from the cell body that were at least twice its length. (C) DRG explants were transfected with Sch-GFP or GFP alone 5 days after plating and were examined 2 and 5 days later. By five days of transfection, Sch-GFP-expressing SCs aligned on axons and were bipolar, whereas GFP-expressing SCs did not align on axons and displayed a flattened, fibroblastic morphology.

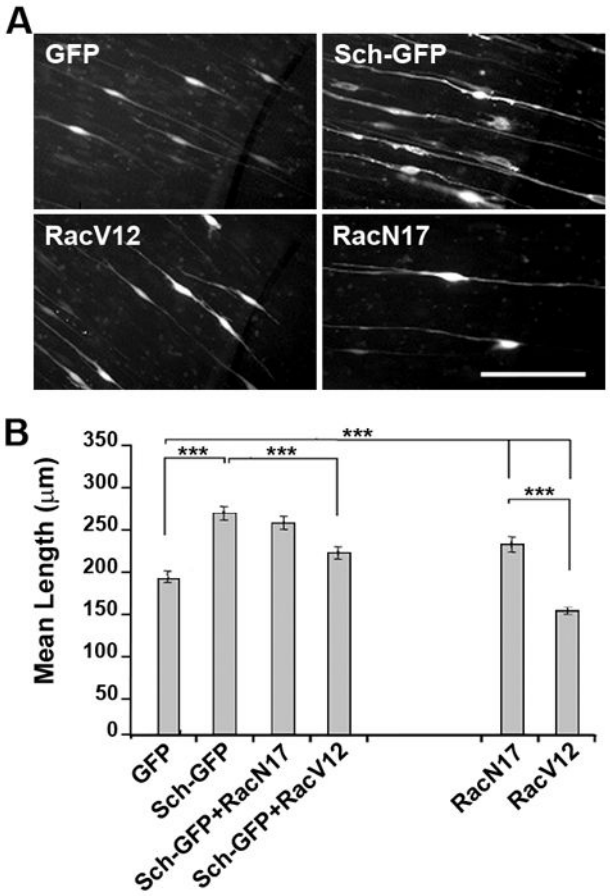

Figure 3. Sch Increases SC Length by Inhibiting Rac Activity

(A) 21 day-old embryonic rat DRG explant cultures were transfected with plasmids encoding GFP or Sch-GFP and HA-tagged dominant negative (RacN17) and constitutively active (RacV12) Rac. GFP-expressing SCs were imaged 3 days after transfection. (B) The total length of GFP-expressing SCs was measured in three experiments and mean and SEM of all cells in each condition is shown. SCs expressing RacN17 (n=224) were significantly longer than those expressing RacV12 (n=230) and were similar in length to Sch-GFP-expressing SCs (n=217) which were 41% longer than GFP controls (n=333). The lengths of SCs co-expressing Sch-GFP with RacN17 (n=213) were not statistically different from SCs expressing Sch-GFP alone. (Sch-GFP/RacV12, n=233). Statistical significance (p-value) between different pairs of transfection/co-transfection conditions was calculated using a paired t-test.

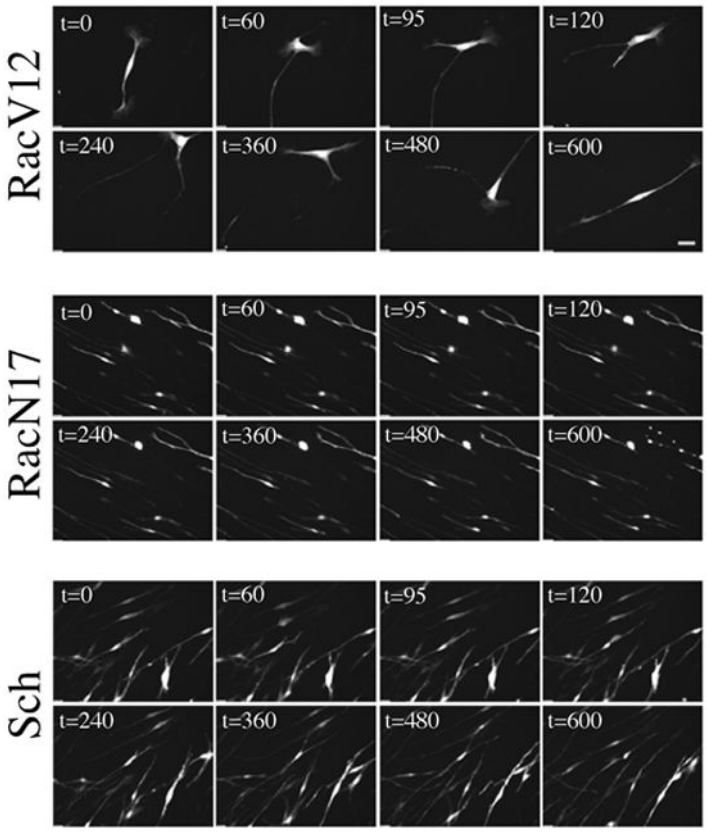

Figure 4. SCs Expressing Sch and RacN17 Undergo Axon-Directed Cellular Elongation

21 day-old embryonic rat DRG explant cultures were co-transfected with plasmids encoding GFP, Sch-GFP and HA-tagged variants of RacV12 or RacN17. Live imaging was performed beginning 36 hours after transfection and continued for 18 hours to visualize GFP expressing SCs. A representative field of cells is shown at the indicated times (minutes). SCs transfected with RacV12 undergo continual transitions in morphology. In contrast, SCs transfected with either RacN17 or Sch remain aligned on axons and slowly elongate. Immunostaining for the HA epitope was conducted after imaging to verify that GFP-expressing SCs also expressed Rac variants (data not shown). Scale bars indicate 10μm. See also Supplemental Movies 1-3.

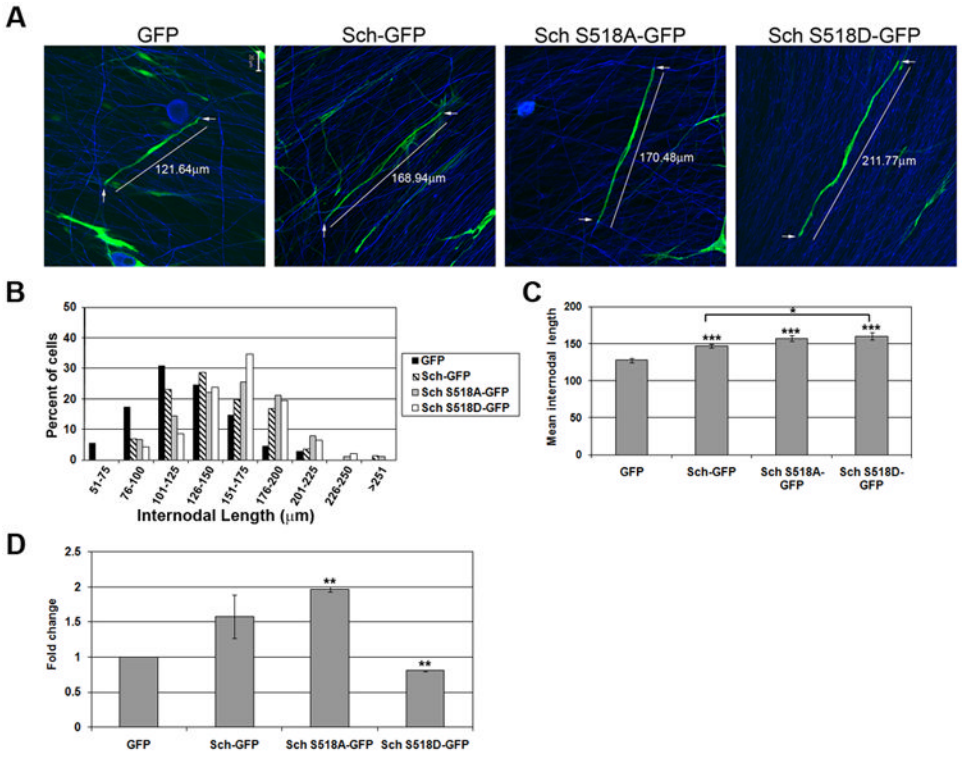

Figure 5. Sch Increases Myelin Segment Length and Myelination Frequency

(A) Dissociated rat DRGN/SC co-cultures were transiently transfected with plasmids encoding GFP, Sch-GFP, GFP-Sch-S518A and GFP-Sch S518D one day prior to addition of M-feed to induce myelination. The co-cultures were immunostained 10-14 days later with antibodies to MAG or Caspr and neurofilament heavy chain to identify myelin segments (not shown). Scale bars indicate 20μm. (B) The histogram depicts the distribution of all GFP-positive myelin segments measured in four experiments. (GFP, n = 110; Sch-GFP, n=141; GFP-Sch-S518A, n=90; GFP-Sch S518D, n=46). (C) The mean internodal length of all segments from 4 independent experiments is shown. (D) The graph represents the mean fold change in the total number of GFP-positive myelinating SCs in 2 independent experiments with equivalent transfection and myelination efficiencies. Error bars represent the SEM. P-values are indicated as follows: (*) ≤0.05, (**) ≤0.005, (***) ≤ 0.0001.

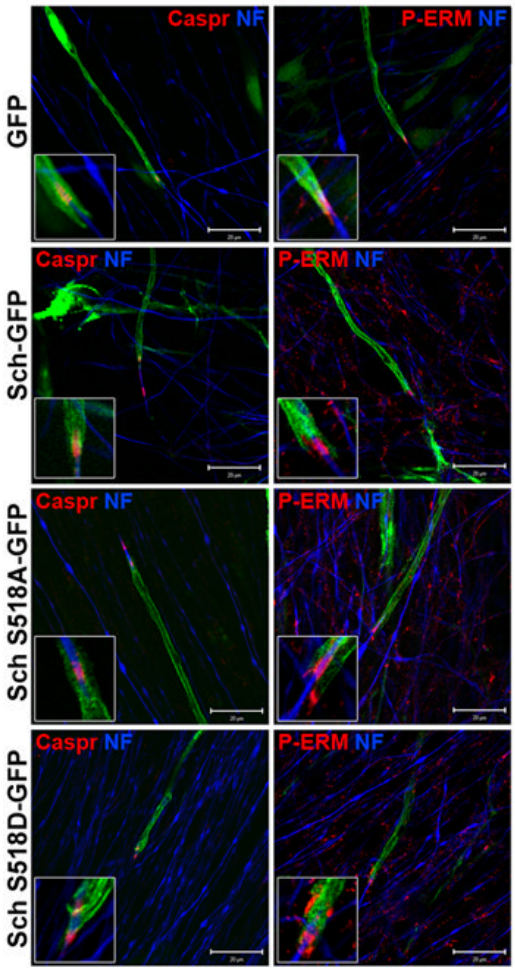

Figure 6. Sch-GFP Expression Does Not Alter Caspr and P-ERM Localization

Rat DRGN/SC co-cultures were transiently transfected with GFP, Sch-GFP and GFP-tagged Sch-S518A/D variants and were induced to myelinate. The co-cultures were immunostained with antibodies against Caspr and P-ERM to assess paranodal and nodal structures, respectively, and neurofilament heavy chain (NF) to visualize axons. Scale bars indicate 20μm and the insets represent a 2x digital zoom of the paranodal-nodal region.

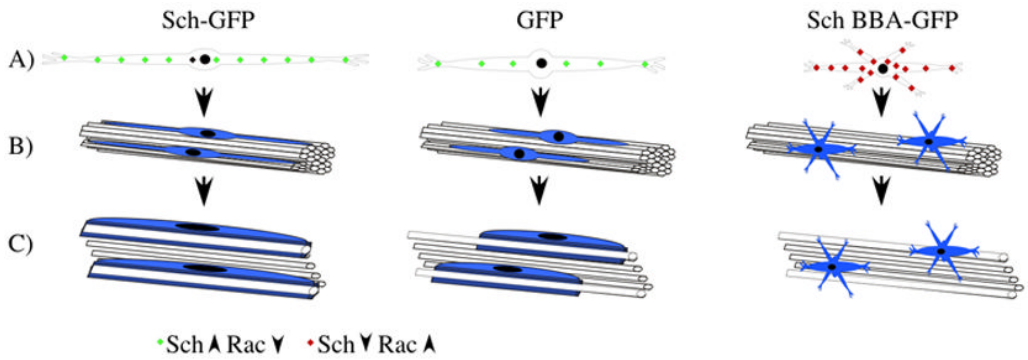

Figure 7. Model of Sch-Dependent Regulation of SC Morphology

The illustration depicts the effect of Sch-GFP, Sch-BBA-GFP and GFP overexpression on: A) SC morphology, B) SC alignment with axons, and C) SC myelination of axons. Our data support the hypothesis that overexpression of Sch reduces Rac GTPase activity at the plasma membrane which leads to formation of elongated bipolar SCs and myelin segments. In contrast, overexpression of the Sch-BBA-GFP dominant-negative variant prevents Sch-mediated inhibition of Rac and results in formation of multipolar SCs unable to align with or myelinate axons.

Table 1

Effect of Sch on SC Process Length

μm	GFP	Sch-GFP	Sch-BBA-GFP
Range	21-562	30-951	28-383
Mode	51-100	151-200	51-100
Mean	140±6	256±11	118±5
*p value		≤0.0001	≤0.005

Range is the greatest of 3 experiments

Mode in each experiment for GFP and Sch-BBA-GFP and in 2 of 3 for Sch-GFP; mode for 3rd experiment is 201-251 μm.

Mean and SEM of all processes from 3 experiments

*compared to GFP using unpaired t test (GraphPad)